

Unicellular Algal Growth: A Biomechanical Approach to Cell Wall Dynamics

Royce Kam and Herbert Levine

Department of Physics, University of California, San Diego, La Jolla, California 92093-0402

(Received 24 April 1997)

We model a growing cell in a calcium solution as an elastic shell on short time scales. The turgor pressure and elastic properties (Young's modulus, thickness) of the cell wall determine a stressed cell shape. Enzyme-mediated relaxation of the unstressed toward the stressed configuration results in a slow (plastic) deformation of the cell. The cell wall thickness is then modulated by calcium-mediated fusion of material and elongation. We analyze small perturbations to a circular cell and find an instability related to modulations of the wall thickness, leading to growth rates which peak at a finite wave number. [S0031-9007(97)04635-8]

PACS numbers: 87.10.+e, 87.22.-q

In recent years, there has been increasing interest in models of unicellular growth. Specific examples include dendritic branching in neuronal growth [1,2] and the broadening and branching of lobes in unicellular algal growth [3–5]. Algal models have ranged from geometrical models (cf. geometric models of dendritic growth in solidification [6]) to those combining the geometric formalism with a diffusive “morphogen” field. At the same time, a wealth of experimental information regarding unicellular morphogenesis has been provided by studies of the larger species of the alga *Micrasterias*. Morphogenesis in *Micrasterias* proceeds by a very well-ordered sequence of tip splitting and lobe broadening, culminating in elegant fan shapes (Fig. 1) reminiscent of patterns seen in unstable diffusion-limited growth [7]. As motivated by these experiments, we have constructed a generic model for cell wall dynamics which we believe will form the basis for realistic models of unicellular morphogenesis.

Although some of the details remain elusive, a general picture of cell growth in algae has emerged from experiment. In order for the cell to elongate without thinning indefinitely, vesicles containing cell wall material are synthesized within the cytoplasm and then travel toward the cell periphery where they fuse with the cell membrane, a process mediated by calcium ions [8]. For example, growing tips of *Micrasterias* exhibit high concentrations of membrane-associated calcium [8,9], enabling them to fuse vesicles in much larger quantities than other areas of the cell wall [10]. Meanwhile, there is evidence that calcium concentration does not vary significantly within the body of the cell itself [11], implying that the relevant diffusive processes occur *outside* the cell body even as they modulate the concentration at the cell wall.

Experiments that halt growth by reducing turgor pressure demonstrate that elongation is (at least in part) a response to the stresses in the cell wall [10]. In addition, it is believed that a “loosening factor” must be present to allow the fibers making up the wall to slip past each other during elongation (e.g., the protein “expansin” [12]) Since most elongation occurs at the cell tips [8,13], we might surmise that high concentrations of calcium also imply

high concentrations of the “loosening” factor. These observations have led us to a simple model for cell wall dynamics in algae.

Consider a cell growing in a solution of calcium ions. Treat the cell wall as an elastic shell on short time scales, whose slow plastic deformation is then governed by a loosening factor. Further, assume that the fusion of vesicles with the cell membrane is also a long time scale process.

We begin by discretizing the stressed shape into N rods (mathematical objects for summing, *not* particular physical elements such as microfibrils) with lengths l_i and orientations θ_i . Likewise, the unstressed shape will consist of N rods with lengths l'_i and orientations θ'_i (and our convention hereafter will be to associate all primed quantities with the unstressed shape). The stressed shape minimizes (subject to the constraint of a closed shape) the energy

$$U = p \sum_{i=1}^N l_i \sin \theta_i \sum_{j=1}^i l_j \cos \theta_j + \sum_{i=1}^N \frac{1}{2} \alpha_i (l_i - l'_i)^2 + \sum_{i=1}^N \frac{1}{2} \beta_i (\kappa_i - \kappa'_i)^2, \quad (1)$$

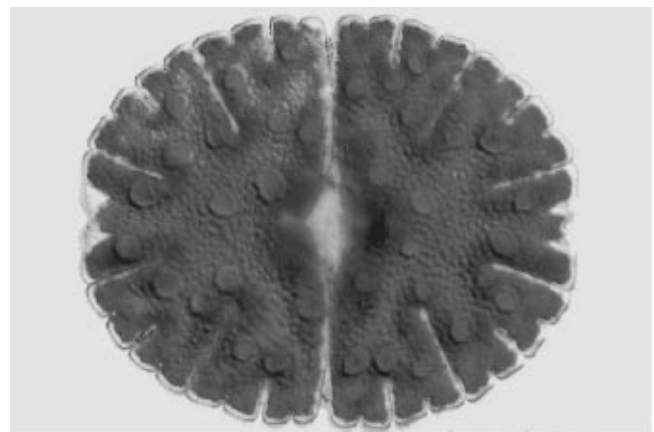


FIG. 1. *Micrasterias denticulata*, diameter $\sim 200 \mu\text{m}$. Picture provided by U. Meindl.

where κ_i is the local curvature. The sums are finite element representations of, respectively, the energy due to the pressure ($p \int x dy$, where $p < 0$ for an outward pressure), the usual strain energy arising from Hooke's law ($\int \frac{1}{2} E h \xi^2 ds$ where $\alpha_i \equiv E h_i / l'_i$, E is Young's modulus, and ξ is the strain), and the pure bending energy of a rod ($\int \frac{1}{2} E I (\kappa - \kappa')^2 ds$ where $\beta_i \equiv E I_i l'_i$ and the moment $I \equiv \int x^2 dx$ integrated over the rod's width for an isotropic material [14,15]). Note that at this stage we wish to create a tractable 2D analog of the actual 3D cell (remembering that 2D models of snowflake growth were able to capture almost all of the salient features of the growth dynamics [7]).

We then quasistatically calculate the calcium concentration on the stressed cell shape. Assuming that diffusion occurs *outside* the cell, we solve $\nabla^2 u = 0$ in that region, where $u \equiv (C - C_\infty) / C_\infty$ is the *normalized* concentration, $C_\infty \equiv C(R_\infty)$, and $u(R_\infty) = 0$ with R_∞ a large, but finite radius. At the cell boundary itself, let the flux through the membrane be $\partial u / \partial n = j(u) / D$, where \mathbf{n} is the *outward* normal, $j(u)$ is the *inward* current, and D is the diffusion constant. In general, we expect *active* pumping mechanisms to dominate the current so that $j(u)$ is independent of the wall thickness (which is not true for a *passive* current through a permeable membrane).

We allow the unstressed shapes to relax toward the stressed configuration via

$$\frac{dl'_i}{dt} = \Gamma(u) (l_i - l'_i), \quad (2)$$

$$\frac{d\theta'_i}{dt} = \Gamma(u) (\theta_i - \theta'_i), \quad (3)$$

where $\Gamma(u)$ is the characteristic relaxation rate as a function of the loosening factor assuming, for simplicity, that it is the equivalent of the calcium concentration. Finally, let $\chi(u)$ be the rate at which mass (equivalently, the area $h_i l'_i$, if the density is uniform) is added per unit length to a given rod through vesicle fusion, then

$$\frac{dh_i}{dt} = \chi(u) - \frac{h_i}{l'_i} \frac{dl'_i}{dt}, \quad (4)$$

which completes the specification of the model.

We now calculate the growth rates of perturbations to a circular cell. We can always choose to parametrize the unstressed membrane by dividing it into N rods of equal length $l'_i = a'_0$. Then $\theta'_i = \pi/2 + \phi_i + b'_1 \delta \sin m \phi_i$ with $\phi_i \equiv 2\pi(i-1)/N$, specifies a perturbed circle with a curvature $\kappa' \approx R_0'^{-1} + m b'_1 R_0'^{-1} \delta \cos m \phi$ where $R_0' \equiv N a'_0 / 2\pi$. We specify the perturbed wall thickness as $h_i = h_0 + h_1 \delta \cos m \phi_i$. The stressed coordinates will then have the form $l_i = a_0 + a_1 \delta \cos m \phi_i$ and $\theta_i = \pi/2 + \phi_i + b_1 \delta \sin m \phi_i$. [Note: Hereafter, F_0 and F_1 will refer to the orders of a function F expanded in δ , $F \equiv F_0 + F_1 \delta \cos m \phi$.]

In the continuum limit, expand the total energy as $U \approx U_0 + \delta^2 U_2$, noting that the $\mathcal{O}(\delta)$ energy vanishes upon integration with respect to ϕ [16]. Minimizing U_0 with respect to a_0 yields a quartic equation for $a_0 \equiv 2\pi R_0 / N$.

$$R_0^4 \left(p + \frac{E h_0}{R_0'} \right) - E h_0 R_0^3 + E I_0 R_0 - E I_0 R_0' = 0. \quad (5)$$

The solution, to $\mathcal{O}(p)$, is $R_0 \approx R_0' - p R_0'^4 / (E h_0 R_0'^2 + E I_0)$. We solve for the perturbations by minimizing U_2 with respect to a_1 and b_1 (a long but straightforward calculation), yielding an answer in terms of a_0 [17].

$$a_1 = (a_0 - a'_0) \frac{p R_0^8 h_1 - (m^2 - 1) E I_0 R_0 R_0' \{ m I_0 R_0 b'_1 + [R_0^3 + \frac{dI}{dh_0} (R_0 - R_0')] h_1 \}}{-p h_0 R_0^8 + (m^2 - 1) E I_0 R_0' [h_0 R_0^4 - I_0 (R_0 - R_0')^2]}, \quad (6)$$

$$b_1 = \frac{m(m^2 - 1) E I_0 R_0 [h_0 R_0^4 - I_0 R_0' (R_0 - R_0')] b'_1 + (R_0 - R_0') \{ p R_0^7 - (m^2 - 1) \mathcal{B} \} h_1}{-m p h_0 R_0^8 + m(m^2 - 1) E I_0 R_0' [h_0 R_0^4 - I_0 (R_0 - R_0')^2]}, \quad (7)$$

where $\mathcal{B} \equiv E R_0^3 (I_0 R_0' - h_0 \frac{dI}{dh_0} R_0) - E I_0 (R_0 - R_0') \times (R_0^3 - R_0' \frac{dI}{dh_0})$, $I_0 \equiv I(h_0)$, and dI/dh_0 is the derivative evaluated at $h = h_0$. Observe that if the bending energy is made to vanish for a cell with uniform thickness (i.e., $I_0 = dI/dh_0 = h_1 = 0$) we find that the stressed shape is a perfect circle ($a_1 = b_1 = 0$). This agrees with the well-known "membrane" result that the tension $T = |p|/\kappa$, implying that curvature variations in a pliable membrane require external support [18].

We must now calculate the concentration on the stressed shape, which by direct integration of $dx_i = l_i \cos \theta_i$ and $dy_i = l_i \sin \theta_i$ is seen to have the radial perturbation $R_1 = R_0 (m b_1 - a_1 / a_0) / (m^2 - 1)$ for $m > 1$ [19]. The unperturbed solution is easily found to be $u_0(r) = R_0 D^{-1} j_0 \ln(r/R_\infty)$ where $j_0 = j(u_0(R_0))$.

Meanwhile, the perturbed solution must have the form $u(r, \phi) \approx u_0(r) + c r^{-m} \delta \cos m \phi$. Applying the flux boundary condition and solving for the concentration at the cell wall, $u(R) \equiv u_0 + u_1 \delta \cos m \phi$, yields [20]

$$u(R) \approx u_0(R_0) + \frac{j_0(m-1)}{mD + R_0 \frac{\partial j}{\partial u_0}} R_1 \delta \cos m \phi, \quad (8)$$

where $\partial j / \partial u_0$ (and like expressions) refers to the derivative evaluated at $u = u_0(R_0)$.

The stressed and unstressed shapes, along with the concentration just calculated, allow us to calculate $l'_i(t + dt)$ and $\theta'_i(t + dt)$ through Eqs. (2) and (3). Reparametrizing the solution at $t + dt$ so that we again have equal length rods [21] yields

$$\frac{db'_1}{dt} = \Gamma_0(b_1 - b'_1) - \frac{\Gamma_0 a_1}{ma'_0} + \frac{\partial \Gamma}{\partial u_0} \frac{\xi_0 u_1}{m}, \quad (9)$$

where $\Gamma_0 \equiv \Gamma(u_0(R_0))$. The rate of wall thickening can be calculated directly from (4) as

$$\begin{aligned} \frac{dh}{dt} = & \chi_0 - h_0 \Gamma_0 \xi_0 \\ & + \left\{ u_1 \left(\frac{\partial \chi}{\partial u_0} - h_0 \frac{\partial \Gamma}{\partial u_0} \xi_0 \right) \right. \\ & \left. - \Gamma_0 \left(h_1 \xi_0 + h_0 \frac{a_1}{a'_0} \right) \right\} \delta \cos m \phi, \quad (10) \end{aligned}$$

where $\chi_0 \equiv \chi(u_0(R_0))$ and $\xi_0 \equiv (a_0 - a'_0)/a'_0$. We have tested these analytic results against simulations of the instantaneous rates and found them to be in agreement, with the error converging as $1/N^2$.

Let us qualitatively examine the instabilities in (9) and (10). Assume that both the relaxation and vesicle fusion rates increase with higher concentrations (i.e., $\partial \Gamma / \partial u_0$, $\partial \chi / \partial u_0 > 0$). Take the bending moment to be $I \propto h^n$ where $n > 1$ and $h \ll R$ [15]. We use $j = u - c_u$ with c_u a constant even though a realistic current is much more complicated. Note that the stressed curvature is $\kappa \approx R_0^{-1} + R_0^{-1}(mb_1 - a_1/a_0)\delta \cos m\phi$.

First, consider a perfectly circular cell that develops a slight thickening of the cell wall at $\phi = 0$ (i.e., $b'_1 = 0$ and $h_1 > 0$). For small pressures we have $b_1 \approx -\xi_0 h_1 (I_0 - h_0 \frac{dI}{dh_0}) / mI_0 > 0$ and $a_1 \approx -h_1 (a_0 - a'_0) / h_0 < 0$. This implies that $\phi = 0$ is a “tip” ($\kappa_1 > 0$), which is also a minimum of strain ($a_1 < 0$). This agrees with experiments showing that wall stresses are minimized at cell tips [22]. Inspection of Eq. (10) yields two instability mechanisms. The first is diffusive in that a tip yields a concentration maximum which fuses vesicles at a higher rate, thus amplifying the initially slight thickening. The second is purely elastic in that a thicker region gives rise to a tip which experiences less stress (and less elongation), causing that region to thin more slowly. This second instability is present even if the relaxation and deposition rates are independent of concentration.

Another interesting case is that of a perturbed cell shape which has a constant thickness (i.e., $b'_1 > 0$ and $h_1 = 0$). To lowest order in pressure, we find that $(b_1 - b'_1) \sim p b'_1 R_0^3 / E h_0^{n-1} (m^2 - 1) < 0$, $a_1 \sim -(a_0 - a'_0) m b'_1 h_0^{n-1} / R_0^2 < 0$, and $\kappa_1 \sim m b'_1$. Again, we find that the minimum strain occurs at the tip. Looking at Eq. (9), we see that $-\Gamma_0 a_1 / m a'_0$ is destabilizing, while $\Gamma_0 (b_1 - b'_1)$ is stabilizing. But since $h \ll R_0$, we expect the net effect to stabilize b'_1 . Apparently, without modulations in the cell wall thickness, tips will be smoothed out. This effect may explain the “lobe broadening” observed in later stages of tip growth, though only full numerical simulations would demonstrate this.

A trivial yet interesting implication of Eq. (10) is the ability to reproduce the observed patterns of deposition

of wall material when the turgor pressure is reduced [10]. Setting $p = 0$ implies that $\xi_0 = a_1 = 0$, so that $dh_1/dt = u_1 \frac{d\chi}{du_0}$. That is, the thickness variations will simply follow the variations in concentration, allowing large amounts of material to collect at tips.

By assuming the coefficients in (9) and (10) vary slowly and letting $b'_1, h_1 \sim \exp(\lambda t)$, we can obtain an expression for the spectrum of quasistatic growth rates. While it is unprofitable to write the expression here, we nonetheless plot the result for a typical set of parameters in Fig. 2. Observe that small-scale disturbances are damped out, with the growth rate peaking at a finite wave number ($m = 10$ for this particular set of parameters). In addition, note that the $m = 1$ perturbation is indeed a “zero mode.”

It is interesting to see that this relatively simple model can exhibit such rich behavior and reproduce several experimentally observed effects. This model has explicitly assumed that reshaping of the cell wall is a relaxational process, wherein turgor pressure deforms the wall while enzymes allow the wall elements to slowly assume these stressed forms as their permanent forms. Perturbation analysis reveals two shape-selecting instabilities (one diffusive and the other elastic), both to be inherited by the three-dimensional generalization required to model a real algal cell. Finally, while our model is purely biomechanical, we hope that future work based on this formalism will help disentangle the biomechanical effects from the genetic mechanisms which must certainly be present in any biological system.

This work has been supported in part by NSF Grant No. DMR94-15460 and by the San Diego Chapter of the ARCS Foundation.

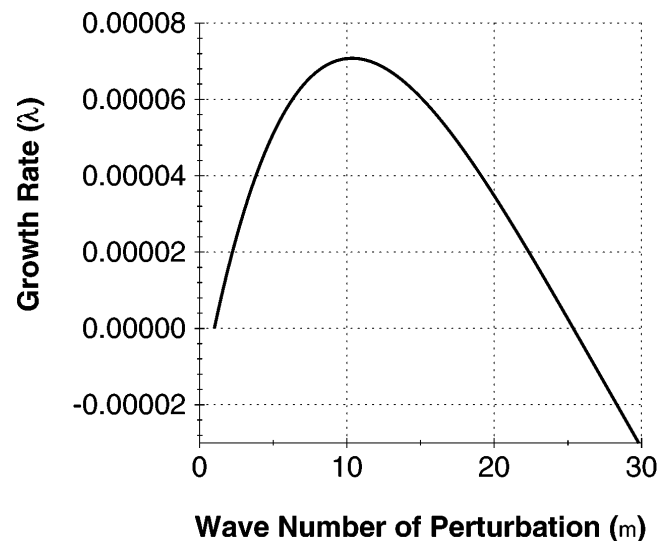


FIG. 2. Spectrum of eigenvalues in the quasistatic approximation. Growth rates (λ) are plotted against wave number (m) for $p = -0.001$, $E = 20.0$, $h_0 = 0.4$, $R'_0 = 10.0$, $R_\infty = 10^6$, $D = 1$, $j = u + 0.15$, $\Gamma = u + 0.15$, and $\chi = 0.20(u + 0.15)$.

- [1] H. G. E. Hentschel and A. Fine, *Phys. Rev. Lett.* **73**, 3592–3595 (1994).
- [2] G. Albinet and P. Pelce, *Europhys. Lett.* **33**, 569–574 (1996).
- [3] P. Pelce and J. Sun, *J. Theor. Biol.* **160**, 375–386 (1993).
- [4] P. Pelce and A. Pocheau, *J. Theor. Biol.* **156**, 197–214 (1992).
- [5] B. Denet, *Phys. Rev. E* **53**, 986–992 (1996).
- [6] R. C. Brower, D. A. Kessler, J. Koplik, and H. Levine, *Phys. Rev. Lett.* **51**, 1111 (1983).
- [7] D. A. Kessler, J. Koplik, and H. Levine, *Adv. Phys.* **37**, 255–339 (1988).
- [8] U. Meindl, *Microbiol. Rev.* **57**, 415–433 (1993).
- [9] U. Meindl, S. Lancelle, and P. Hepler, *Protoplasma* **170**, 104–114 (1992).
- [10] O. Kiermayer, in *Cytomorphogenesis in Plants*, edited by O. Kiermayer (Springer-Verlag, Wien, New York, 1993), pp. 147–189.
- [11] A. Holzinger, D. Callaham, P. Hepler, and U. Meindl, *Eur. J. Cell Biol.* **67**, 363–371 (1995).
- [12] D. Cosgrove, *BioEssays* **18**, 533–540 (1996).
- [13] M. Nishimura and K. Ueda, *J. Cell Sci.* **31**, 225–231 (1978).
- [14] L. D. Landau and E. M. Lifshitz, *Theory of Elasticity* (Pergamon Press, London, 1959), pp. 75–79.
- [15] For our 2D rod, $I_i = h_i^3/12$.
- [16] The perturbation to the area is $A_1 = -\frac{1}{2}\pi R_0^2(mb_1 - a_1/a_0)^2/(m^2 - 1)$ for $m > 1$, and $A_1 = -\frac{1}{8}\pi R_0^2(b_1 - a_1/a_0)^2$ for $m = 1$.
- [17] For $m = 1$, the total y displacement $\propto (b_1 - a_1/a_0)$. To ensure a closed shape, we impose $b_1 = a_1/a_0$. Minimization yields $a_1 = -h_1(a_0 - a_0')/h_0$, which agrees with the limit $m \rightarrow 1$ of Eq. (6).
- [18] C. R. Calladine, *Theory of Shell Structures* (Cambridge University Press, Cambridge, 1983), pp. 80–86.
- [19] For $m = 1$, explicit integration of $x(\phi)$ and $y(\phi)$ shows that $R_1 = \frac{1}{2}R_0(b_1 + a_1/a_0)$.
- [20] Observe that $u_1 = 0$ for $m = 1$, though technically, we have not required the perturbation to vanish at $r = R_\infty$.
- [21] Given $l = A_0 + A_1\delta \cos m\phi$ and $\theta = \pi/2 + \phi + B_1\delta \sin m\phi$, the equal-length parametrization yielding the same curvature has $A_{0,\text{new}} = A_0$ and $B_{1,\text{new}} = B_1 - A_1/mA_0$.
- [22] Z. Hejnowicz, B. Heinemann, and A. Sievers, *Z. Pflanzenphysiol. Bd.* **81**, 409–424 (1977).